

UC Berkeley

UC Berkeley Previously Published Works

Title

Relationship between Segregation Strength and Permeability of Ethanol/Water Mixtures through Block Copolymer Membranes

Permalink

<https://escholarship.org/uc/item/7hp6d47x>

Journal

Macromolecules, 46(24)

ISSN

0024-9297

Authors

Ozcam, A Evren
Petzetakis, Nikos
Silverman, Skyler
et al.

Publication Date

2013-12-23

DOI

10.1021/ma401957s

Peer reviewed

Relationship between Segregation Strength and Permeability of Ethanol/Water Mixtures through Block Copolymer Membranes

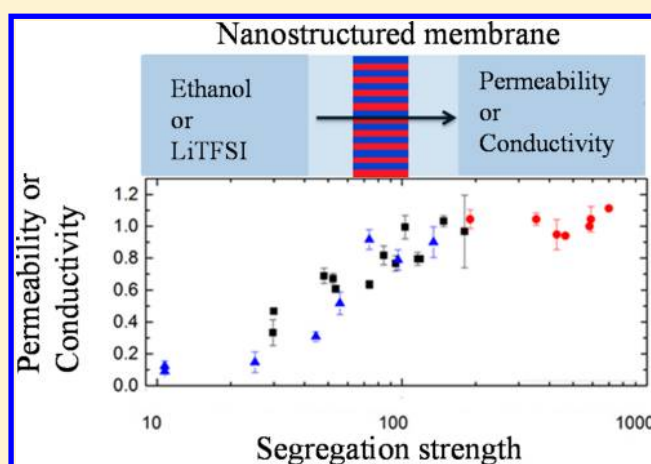
A. Evren Ozcam,[†] Nikos Petzetakis,[†] Skyler Silverman,[‡] Ashish K. Jha,[†] and Nitash P. Balsara^{*,†,§}

[†]Department of Chemical & Biomolecular Engineering, University of California, 201 Gilman Hall, Berkeley, California 94720, United States

[‡]Department of Materials Science & Engineering, University of Pennsylvania, 3231 Walnut Street, Philadelphia, Pennsylvania 19104, United States

[§]Materials Sciences Division & Environmental Energy Technologies Division, Lawrence Berkeley National Laboratory, University of California, 1 Cyclotron Road, Berkeley, California 94720, United States

ABSTRACT: A series of poly(styrene-*b*-dimethylsiloxane-*b*-styrene) (SDS) triblock copolymers with molecular weights ranging from 55 to 150 kg/mol and polydimethylsiloxane (PDMS) volume fractions ranging from 0.59 to 0.83 were used to fabricate membranes for ethanol/water separation by pervaporation. The rigid polystyrene (PS) microphase provides the membrane with structural integrity, while the rubbery PDMS microphase provides nanoscale channels for ethanol transport. We use a simple model to study the effect of morphology and PDMS volume fraction on permeabilities of ethanol and water through the block copolymer membranes. We defined normalized permeabilities of ethanol and water to account for differences in morphology and PDMS volume fraction. We found that the normalized ethanol permeability in SDS copolymers was independent of the total polymer molecular weight. This is qualitatively different from what was previously reported for poly(styrene-*b*-butadiene-*b*-styrene) (SBS) membranes, where the normalized ethanol permeability was found to be a sensitive function of total molecular weight [*J. Membr. Sci.* **2011**, *373*, 112]. We demonstrate that this is due to differences in the Flory–Huggins interaction parameter (χ) for the two systems. When χN is less than 100 (N is the number of segments per chain), the two microphases are weakly segregated, and the presence of glassy PS segments in the transporting microphase impedes ethanol transport. When χN exceeds 100, the two microphases are strongly segregated and the glassy PS segments do not mix with the transporting phase. We compare these results with normalized ionic conductivity data previously reported for mixtures of a lithium salt and polystyrene-*b*-poly(ethylene oxide) (SEO). Evidence suggests that the product χN governs the transport of widely different species such as ethanol and lithium salts through block copolymer membranes. Surprisingly, the normalized permeability of water is independent of total molecular weight for both SDS and SBS block copolymers.



1. INTRODUCTION

Biofuel production using lignocellulosic (LC) feedstock is one of the most promising renewable energy resources. Conventionally, fuel-grade bioethanol with ethanol content in excess of 99 wt % is obtained in two steps. First, the LC feedstock is fermented to give a complex solution containing 3 to 8 wt % ethanol. In the second step, distillation and dehydration are used to increase the ethanol content. The amount of energy consumed in the second step is a significant fraction of the total energy extracted from biofuels. It is recognized that pervaporation can, in principle, reduce the energy required for biofuel purification, and thus it can make the overall biofuel production more efficient.^{1,2}

Pervaporation is a membrane-based separation process that is used to separate liquid mixtures under mild operating

conditions. First, the feed solution sorbs on the feed side of the membrane according to its partition coefficient between the aqueous and membrane phase. It then diffuses through the membrane and evaporates at the permeate side due to low downstream pressure. The composition of the permeate depends on the permeability of the feed components through the membrane and the thermodynamic properties of the liquid and vapor phases.³

Several previous studies have investigated pervaporation through polymeric membranes.^{4–16} This paper is part of a series on the use of microphase-separated block copolymers for

Received: September 24, 2013

Revised: November 17, 2013

Published: December 2, 2013

pervaporation of ethanol/water mixtures.^{12,13} In our studies, we employ block copolymer membranes, where one of the components is chosen to promote ethanol transport while the other is chosen to provide the membrane with structural integrity. Furthermore, the size and shape of the pathways of transport are tuned by changing the molecular weight and composition of the employed block copolymers. It is perhaps worth noting that similar strategies are used to design mechanically robust membranes for ion transport.^{17–20} While, in general, the transporting channels can be aligned via application of external fields, in our work, we used randomly oriented domains obtained without the use of external fields.

To our knowledge, ref 13 is the first systematic study on the effect of block copolymer composition and molecular weight on ethanol/water pervaporation.¹³ The block copolymers used in that study were a series of poly(styrene-*b*-butadiene-*b*-styrene) (SBS) triblock copolymers (polystyrene, PS, is the structural microphase and polybutadiene, PBD, is the ethanol-transporting microphase). Interestingly, it was found that ethanol permeability, P_E , was a strong function of block copolymer molecular weight at fixed volume fraction of the transporting PBD block, ϕ . In contrast, water permeability, P_w , was a weak function of block copolymer molecular weight at fixed ϕ . Herein, we report on the pervaporation of ethanol/water mixtures through poly(styrene-*b*-dimethylsiloxane-*b*-styrene) (SDS) membranes. Our work was motivated by the fact that previous studies have shown that cross-linked polydimethylsiloxane (PDMS) membranes are more effective for ethanol/water pervaporation relative to cross-linked PBD membranes. In this study, we show that the pervaporation characteristics of SDS membranes are very different from those of SBS membranes previously reported. We propose that these differences arise due to differences in the Flory–Huggins interaction parameters that govern microphase separation in the two systems.

2. EXPERIMENTAL SECTION

2.1. Polymer Synthesis and Characterization. The synthetic route used to synthesize the SDS copolymers is summarized in Figure 1. *sec*-Butyl lithium (*sec*-BuLi), dibutyl magnesium (DBM), calcium hydride (CaH_2), 2-methoxyethylether (diglyme), and dichlorodimethylsilane were purchased from Aldrich and used as received. The rest of the chemicals were purified by using high vacuum techniques unless otherwise stated.²¹

Cyclohexane was purchased from Aldrich and was purified by a commercial solvent purification system (Braun, MB AUTO-SPS

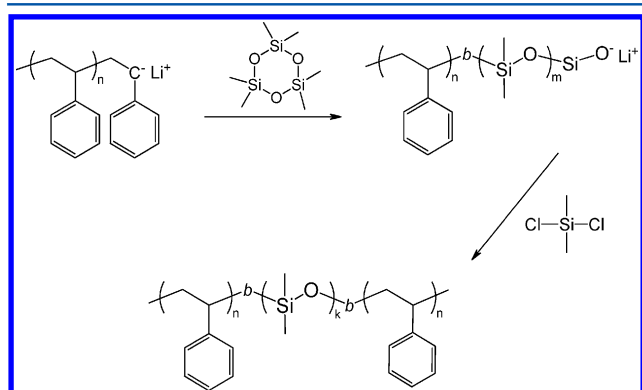


Figure 1. Reaction scheme for synthesis of SDS triblock copolymers via sequential anionic polymerization of styrene and hexamethylcyclotrisiloxane and subsequent coupling with dichlorodimethylsilane.

Solvent Purification System), followed by stirring over polystyryl lithium anions overnight to remove trace amounts of water. Styrene was purchased from Aldrich and was purified by stirring over freshly powdered CaH_2 overnight at room temperature, followed by stirring over a DBM solution at room temperature for 12 h. Hexamethylcyclotrisiloxane (D_3) monomer was purchased from Gelest and was dissolved in freshly distilled cyclohexane (dried as previously mentioned) and left to stir overnight in the presence of freshly powdered CaH_2 . Subsequently, the D_3 /cyclohexane mixture was vacuum transferred to another reactor containing DBM and left to stir at room temperature overnight. Polymerization of styrene was initiated by the addition of *sec*-BuLi and was performed at room temperature for ~ 12 h. After completion of the styrene polymerization, an aliquot of the reaction mixture was isolated and terminated for characterization purposes. Subsequently, predetermined amounts of D_3 and cyclohexane were transferred to the reactor containing living polystyryl lithium. Diglyme was added to the reaction mixture (~ 5 vol %) to facilitate the polymerization of the D_3 monomer. The reaction was conducted at room temperature for 3–5 h. The polymerization of D_3 was stopped at low conversion (~ 30 – 40%) to avoid side reactions and to obtain well-defined diblock copolymers. Aliquots were extracted from the reaction mixture and terminated with degassed isopropanol for characterization purposes. Typical characterization data obtained during polymerization are shown in Figure 2, where we show gel

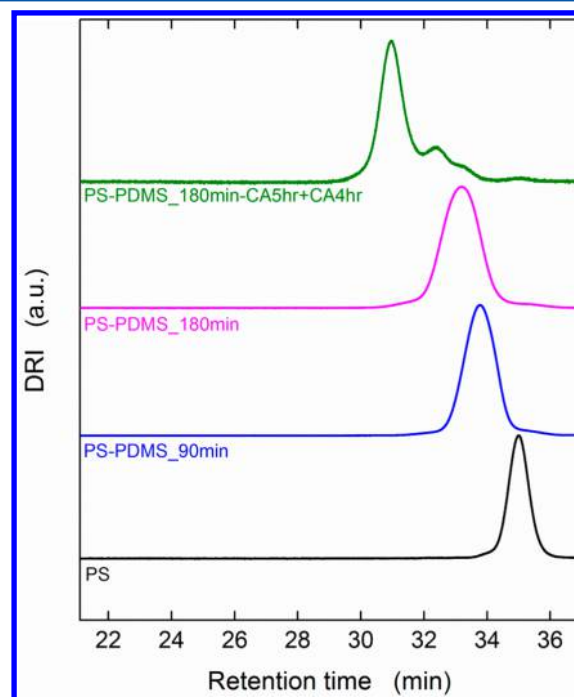


Figure 2. Gel permeation chromatographs of the polystyrene (PS) precursor, PS-PDMS diblock copolymers during polymerization (90 min) and after completion of polymerization just before the addition of the coupling agent (180 min), and the SDS triblock copolymer.

permeation chromatographs obtained from the PS homopolymer and the PS-*b*-PDMS diblock copolymer after 90 and 180 min (blue and purple trace, respectively) of D_3 propagation. These data were obtained during polymerization of SDS117-83 (block copolymers are named SDSXX-YY, where XX is the number-averaged molecular weight of the sample in kilograms per mole and YY is the volume fraction of the PDMS block).

SDS triblock copolymers were obtained by introducing stoichiometric amounts of dimethyldichlorosilane. Degassed isopropanol was added to the reactor to terminate the remaining uncoupled living chains, and the polymerization mixture was precipitated in a 50 vol % methanol and isopropanol mixture.²² The copolymers were purified by two additional precipitation steps (dissolution in THF, followed by

Table 1. Characteristics of the SDS Triblock Copolymers Used in This Study

	ϕ_{PDMS}	M_n (kg/mol)	$\text{PDI}_{\text{diblock}}$	coupling ratio (wt %)	d spacing (nm)	morphology
SDS117-83	0.83	10.9–95.6–10.9	1.06	100	46.3	cylindrical
SDS87-82	0.82	8.5–70.0–8.5	1.06	100	37.9	cylindrical
SDS55-78	0.78	6.5–42.0–6.5	1.08	81.9	28.3	cylindrical
SDS150-73	0.73	21.7–106.5–21.7	1.03	70.3	56.4	cylindrical
SDS148-72	0.72	22.0–104.0–22.0			61.9	cylindrical
SDS90-69	0.69	15.0–60.0–15.0			43.8	lamellar
SDS110-59	0.59	23.5–63.3–23.5	1.05	90.0	51.9	lamellar

precipitation in methanol/isopropanol), followed by filtration of THF polymer solutions before last precipitation. After the last precipitation, copolymers were collected via filtration and dried under vacuum until constant weight was achieved. The gel permeation chromatograph of SDS117-83 obtained after termination and purification is shown in Figure 2. It is evident that our final products contain non-negligible amounts of uncoupled diblock copolymers and other products due to side reactions. The PDMS block molecular weight reported in Table 1 was determined by ^1H NMR spectroscopy using the PS precursor molecular weight.

Our synthetic procedure is based on previous work by Maheshwari et al.²²

The characteristics of the SDS triblock copolymers used in this study are summarized in Table 1. The molecular weights of the PS blocks were determined by GPC (Viscotek with THF as the solvent) based on PS standards. The ratio of PS to PDMS monomeric units in each sample was determined by ^1H NMR spectroscopy with deuterated chloroform as the solvent. The polydispersities of the PS-*b*-PDMS diblock copolymers before coupling, listed in Table 1, were determined by GPC based on PS standards. All of the polymers in Table 1 were synthesized using the procedure previously described with the exception of SDS148-72 and SDS90-69 which were purchased from Polymer Source. The weight ratio of SDS triblock copolymer to the uncoupled PS-*b*-PDMS diblock copolymer precursor in each sample was determined by calculating the areas under the peaks of diblock and triblock portions of the product from the GPC traces (DRI detector). The volume fractions of the PDMS block (i.e., ethanol transporting block) of the SDS copolymers (ϕ_{PDMS}) were estimated using monomer volumes of 0.179 and 0.138 nm³ for PS and PDMS, respectively.²³

2.2. Membrane Preparation. The membranes for pervaporation experiments were prepared by melt pressing the SDS polymers between polytetrafluoroethylene (PTFE) sheets (5 mil thickness, McMaster). SDS copolymer was weighed (1 g), and the pieces of the copolymer were sandwiched between two PTFE sheets. The sandwich was placed between the plattens of a Carver press at 150 °C and 1000 psi for 15 min to obtain films ranging from 100 to 150 μm in thickness. The SDS films were separated from the PTFE sheets, placed on a filter paper (support), and “punched” with a circular punch to obtain a supported membrane with a diameter of 7.5 cm. A few solvent-cast SDS membranes were also prepared as described in ref 12 to compare the pervaporation characteristics of melt-pressed and solvent-cast membranes. The pervaporation characteristics of melt-pressed and solvent-cast membranes were within experimental error.

2.3. Pervaporation Experiments. Pervaporation experiments of ethanol/water mixtures were conducted on a laboratory bench test unit built by Sulzer Chemtech, Germany. The membrane was held inside a circular cell restrained with an O-ring, providing a total permeation area of 37 cm². The temperature of the feed was controlled in the range of 40 \pm 1 °C. Each experiment began with \sim 2 L of 8 wt % alcohol/water solution in the feed tank. On the permeate side of the membrane, a vacuum of 2 to 3 mbar was applied using a vacuum pump (Welch, model 2014), and permeates were condensed in a trap cooled with a dry ice/isopropanol mixture at -80 °C. After the feed pump was started, the system was allowed to attain steady state for 1 h before permeate samples were collected. For each polymer, two different membranes were prepared and pervaporation experiments were repeated twice for each membrane. The average values of the four

runs are reported, and the standard deviation is taken to be the uncertainty of the measurements.

Permeate samples were weighed to determine the mass permeated through the membrane during the experiment. The feed composition was fixed at 8 wt % ethanol. Changes in feed composition due to pervaporation are negligible due to small amounts permeating through the membrane. Flux of either water or ethanol was calculated using the equation

$$J_i = \frac{M_i}{A\Delta\tau_c} \quad (1)$$

where M_i is the mass of individual permeant, A is the permeation area (37 cm²), and $\Delta\tau_c$ is the permeate collection time; subscript E implies ethanol, while subscript W implies water. Membrane permeability, P_i , was calculated from the following equation^{2,24,25}

$$P_i = \frac{J_i t}{(x_i \gamma_i p_i^{\text{sat}} - y_i p_p)} \quad (2)$$

where t is the membrane thickness, x_i is the feed mole fraction, γ_i is the activity coefficient, p_i^{sat} is the saturated vapor pressure, y_i is the permeate mole fraction, and p_p is the permeate pressure. Values of γ_i were determined by analyzing permeate samples by ^1H NMR spectroscopy with deuterated acetone (acetone- d_6) as the solvent. The activity coefficients were calculated using the Van Laar coefficients obtained from ref 26, and the saturated vapor pressure p_i^{sat} was determined using the Antoine equation.²⁷ The ethanol selectivity of the membrane is defined as²⁸

$$\alpha_{\text{EW}} = \frac{P_{\text{E}}}{P_{\text{W}}} \quad (3)$$

We use units of mol m/(m² s Pa) in this paper when we report P_{E} or P_{W} . In some papers (e.g., ref 29), ethanol selectivity is quantified by specifying the overall process separation factor, which is equal to $[y_{\text{E}}(1 - x_{\text{E}})]/[(1 - y_{\text{E}})x_{\text{E}}]$. The process separation factor for our experiments can be obtained by multiplying α_{EW} by 10.6.

3. RESULTS AND DISCUSSION

Figure 3 shows typical SAXS profiles of selected SDS membranes at room temperature. The SAXS profiles were isotropic, indicating that the membrane preparation process led to randomly oriented grains. All of the SAXS profiles contained a primary peak at scattering vector $q = q^*$. In addition, the profiles contained second-order peaks or shoulders at either $q = 2q^*$ or $q = \sqrt{3}q^*$, which are signatures of microphase-separated lamellar and cylindrical morphologies, respectively. The cylindrical morphology comprises PS cylinders arranged on a hexagonal lattice in a PDMS matrix. SAXS patterns collected at high temperatures (up to 200 °C) were indistinguishable from the room-temperature profiles. The domain spacing, d , of each one of the microphase-separated block copolymer membranes was calculated by the equation $d = 2\pi/q^*$.

In Figure 4, we plot the calculated d values as a function of M_n , the total molecular weight of the SDS copolymers. It is evident that d increases with increasing M_n , and the

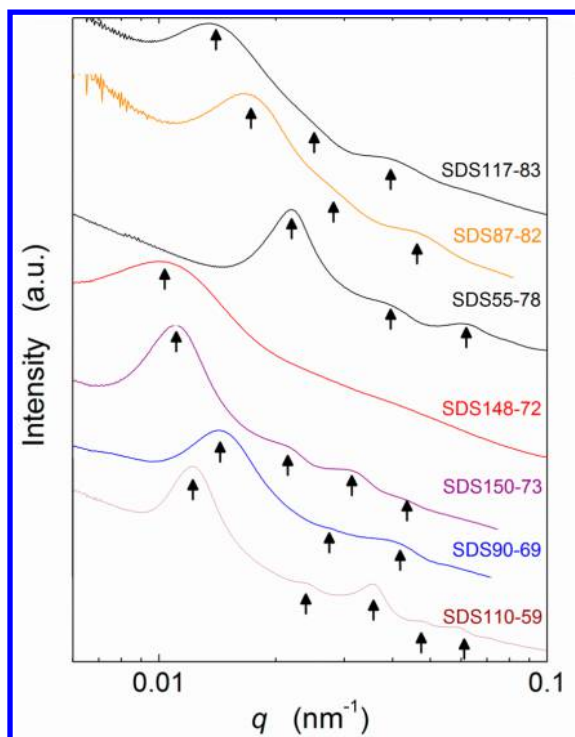


Figure 3. SAXS profiles of microphase-separated SDS triblock copolymers. Scattering intensity is plotted as a function of the magnitude of the scattering vector, q .

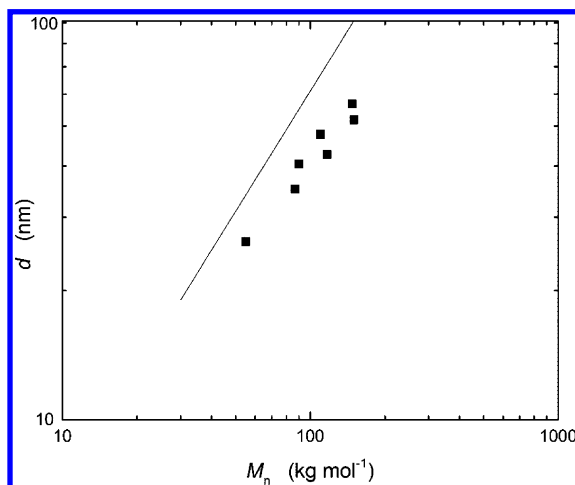


Figure 4. Domain spacing versus total number average block copolymer molecular weight. Scaling law $d \sim M_n^{0.67}$ is represented by the solid line.

experimental data plotted are consistent with this scaling law observed in the strong segregation limit, $d \approx M_n^{0.67}$. The line in Figure 4 represents the expected power law.

In Figure 5, we show the dependence of ethanol and water permeabilities on PDMS volume fraction, ϕ_{PDMS} . We expect permeability through microphase-separated block copolymer membranes to be proportional to the volume fraction of the transporting phase. Therefore, ethanol and water permeabilities have been normalized with ϕ_{PDMS} (P_E/ϕ_{PDMS} and P_W/ϕ_{PDMS}), which accounts for the different volume fraction of PDMS in each block copolymers. The P_E/ϕ_{PDMS} and P_W/ϕ_{PDMS} values for SDS membrane with $\phi_{\text{PDMS}} = 0.59$ were $(6.9$ and $9.5) \times 10^{-12}$ mol m/m² s Pa, respectively. P_E/ϕ_{PDMS} and P_W/ϕ_{PDMS}

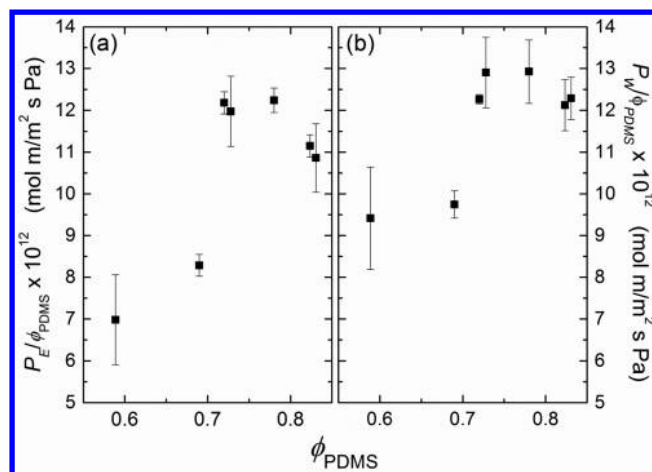


Figure 5. Ethanol (a) and water (b) permeabilities normalized by PDMS volume fraction as a function of PDMS volume fraction.

increased with increasing ϕ_{PDMS} and reached values of $(12$ and $13) \times 10^{-12}$ mol m/m² s Pa for the SDS membranes with ϕ_{PDMS} of 0.72. Samples with lamellar morphology ($\phi_{\text{PDMS}} < 0.7$) exhibit lower P_i/ϕ_{PDMS} ($i = E$ or W) normalized permeabilities than those with cylindrical morphology ($\phi_{\text{PDMS}} > 0.7$).

The dependence of membrane separation factor, α_{EW} , on ϕ_{trans} is shown in Figure 6. It is evident from these data that

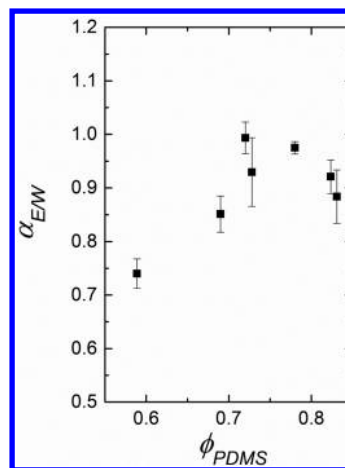


Figure 6. Ethanol selectivity as a function of PDMS volume fraction.

α_{EW} is not a strong function of morphology in this system. The membrane separation factor for SDS membranes ranges from 0.85 to 1.0 for all samples except the membrane with a PDMS volume fraction of 0.59. The concentration of the permeate obtained from optimized SDS membranes with $\alpha_{EW} = 1.0$ is 42 wt % ethanol (feed is 8 wt % ethanol).

Following our previous work on transport through block copolymer membranes, permeability through a strongly microphase-separated block copolymer can be expressed as

$$P_i = f \phi_{\text{trans}} P_{i,o} \quad (i = E \text{ or } W) \quad (4)$$

where ϕ_{trans} is the volume fraction of the transporting phase, $P_{i,o}$ is the intrinsic permeability of the pure transporting phase, and f is a factor that accounts for the morphology of the microphase-separated block copolymers. For cylindrical systems, $f = 1$ because we have a continuous transporting phase.

For lamellar systems, $f = 2/3$ because, on average, one-third of the lamellar grains will be oriented perpendicular to the direction of transport. Equation 4 assumes that transport occurs exclusively in one of the microphases.

If the block copolymer is not strongly microphase separated and transport is restricted to one of the microphases, then the permeability of component i is given by the following equation:

$$P_i = f\phi_{\text{trans}} P_{i,\text{om}}, \quad (i = E \text{ or } W) \quad (5)$$

where $P_{i,\text{om}}$ is the permeability of the mixed transporting phase that now contains segments of the structural block. It is obvious that $P_{i,\text{om}}$ is less than $P_{i,o}$, but one expects $P_{i,\text{om}}$ to approach $P_{i,o}$ as the strong segregation limit is approached.

Segregation in block copolymers primarily depends on two parameters: the Flory–Huggins interaction parameter, χ , and the total number of monomeric units per chain, N . We use a reference volume of 0.1 nm^3 for calculating both χ and N . The values of χ at 40°C for PS/PBD and PS/PDMS are 0.047 and 0.226, respectively.²³ In Table 2, we list the values of χN for the SDS polymers listed in Table 1 and the SBS polymers studied in our previous publication.¹³

Table 2. Morphology Factors (f), χN , and Microphase-Separated Morphology of SDS and SBS Copolymers

name	f	χN	morphology
SDS117-83	1	189.9	cylindrical
SDS87-82	1	353.4	cylindrical
SDS55-78	1	428.4	cylindrical
SDS150-73	1	464.7	cylindrical
SDS148-72	1	582.5	cylindrical
SDS90-69	2/3	590.9	lamellar
SDS110-59	2/3	698.9	lamellar
SBS106-93	1	29.8	spherical
SBS166-93	1	30.0	spherical
SBS34-80	1	48.1	cylindrical
SBS62-80	1	53.6	cylindrical
SBS118-80	1	52.3	cylindrical
SBS207-80	1	73.6	cylindrical
SBS35-73	1	84.3	cylindrical
SBS56-73	1	94.3	cylindrical
SBS98-73	1	102.9	cylindrical
SBS135-73	1	116.1	cylindrical
SBS62-63	2/3	118.5	cylindrical
SBS88-63	2/3	147.8	cylindrical
SBS140-63	2/3	180.1	cylindrical

In Figure 7, we plot $P_i/f\phi_{\text{trans}}$ ($i = E$ and W) as a function of χN for both SDS and SBS copolymers. There are two main features that distinguish data obtained from SDS and SBS systems: (1) $P_i/f\phi_{\text{trans}}$ through SDS membranes is an order of magnitude higher than that through SBS membranes. We attribute this to differences in $P_{i,o}$ values. It is evident from the literature that ethanol permeability through PDMS is much higher than that through PBD.^{30,31} (2) $P_E/f\phi_{\text{trans}}$ through SDS membranes is independent of χN , while that through SBS membranes is not. We propose that this is due to differences in segregation strength.

To further analyze our results, we define normalized permeability, $P_{i,n}$, as

$$P_{i,n} = \frac{P_i}{f\phi_{\text{trans}} P_{i,o}} \quad (6)$$

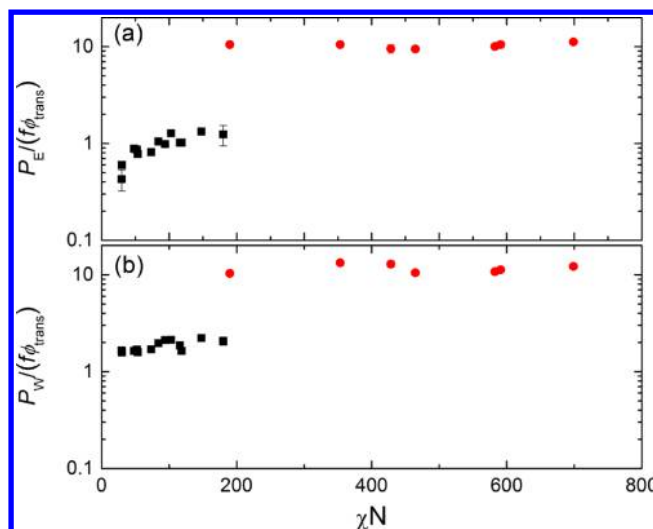


Figure 7. Ethanol (a) and water (b) permeability normalized by the product $f\phi_{\text{trans}}$ where f is the morphology factor and ϕ_{trans} is the volume fraction of the transporting phase for SDS (red circles) and SBS (black squares) membranes as a function of χN where χ is the Flory–Huggins interaction parameter and N is the number of segments per chain.

In Figure 8, we plot $P_{i,n}$ versus χN for both SBS and SDS systems. We use values $P_{E,o} = 1.28 \times 10^{-12}$ and $P_{W,o} = 2.14 \times$

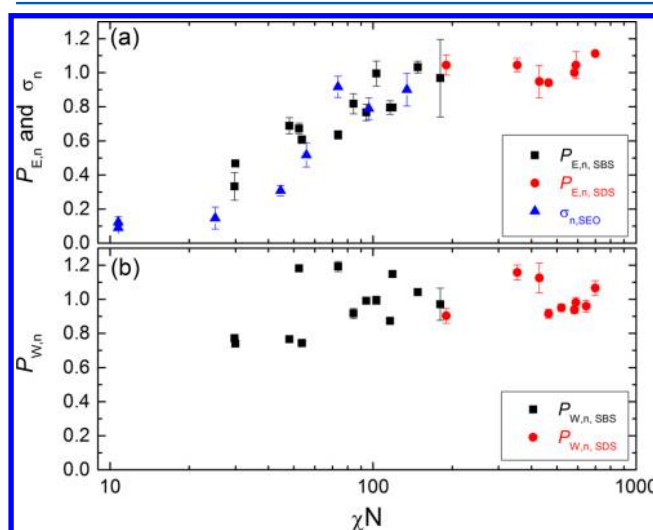


Figure 8. (a) Normalized ethanol permeability through SDS and SBS membranes and normalized ionic conductivity through SEO membranes as a function of χN . (b) Normalized water permeability through SDS and SBS membranes as a function of χN .

10^{-12} for SBS and $P_{E,o} = 10.1 \times 10^{-12}$ and $P_{W,o} = 11.5 \times 10^{-12}$ for SDS [units of permeability are $\text{mol m}/(\text{m}^2 \text{ s Pa})$]. These values were chosen so that $P_{i,n}$ values approached unity in the large χN limit. This follows from the expectation that $P_{i,\text{om}}$ approaches $P_{i,o}$ in this limit. It is evident that the pervaporation data obtained from both SDS and SBS systems collapse on a master curve when $P_{i,n}$ is plotted versus χN . (See Figure 8.) As seen in Figure 8a, $P_{E,n}$ increases from about 0.3 to 1.0 as χN increases from 30 to 100. $P_{E,n}$ is independent of χN when χN exceeds 100. At low values of χN , one expects mixing between the structural (PS) and the transporting (PBD or PDMS) blocks. The presence of glassy PS segments in the transporting

PBD-rich microphase will impede the diffusion of ethanol. The data in Figure 8 suggest that this impediment does not exist when χN exceeds 100. Self-consistent field theory calculations indicate that the morphology of diblock copolymers of a given composition is independent of chain length when χN exceeds 100.³² This independence is one of the signatures of the strong segregation limit in block copolymers and suggests that the strong segregation limit is reached when χN is 100.³³ $P_{E,n}$ is independent of χN for all of the SDS samples (Figure 8a) because χN exceeds 100 in all cases.

It is instructive to compare $P_{i,o}$ values reported above with literature values of permeabilities through cross-linked homopolymers (see Table 3). The permeabilities of ethanol and

Table 3. $P_{E,o}$ and $P_{W,o}$ Values for Different Membranes

membrane	$P_{E,o}$	$P_{W,o}$	temperature
SDS	10.1	11.5	40 °C
cross-linked PDMS	6.00	10.2	50 °C from ref 31
SBS	1.28	2.14	40 °C
cross-linked PBD	0.48	1.81	25 °C from ref 30

water in cross-linked PBD are 0.48×10^{-12} and 1.81×10^{-12} mol m/(m² s Pa).³⁰ These values should be compared with $P_{E,o} = 1.28 \times 10^{-12}$ and $P_{W,o} = 2.14 \times 10^{-12}$ mol m/(m² s Pa) for SBS. The permeability of ethanol and water in cross-linked PDMS are 6.0×10^{-12} and 10.2×10^{-12} mol m/(m² s Pa).³¹ These values should be compared with $P_{E,o} = 10.1 \times 10^{-12}$ and $P_{W,o} = 11.5 \times 10^{-12}$ mol m/(m² s Pa) for SDS. It is interesting to note that the permeability of water in cross-linked PBD and cross-linked SDS homopolymers is similar to the value of $P_{W,o}$ determined from our experiments on block copolymers. In contrast, the permeability of ethanol in cross-linked PBD and cross-linked SDS homopolymers is two times lower than the $P_{E,o}$ determined from our experiments on block copolymers.

It is perhaps worth noting that the dependence of $P_{E,n}$ on χN seen in Figure 8a is very similar to the dependence of the normalized ionic conductivity, σ_n , of mixtures of polystyrene-*b*-poly(ethylene oxide) (SEO), block copolymers, and lithium bis(trifluoromethane)sulfonimide (LiTFSI) on χN .¹⁸ In ref 18, Yuan et al. reported on the ionic conductivity, σ , of SEO/LiTFSI mixtures as a function of SEO molecular weight. In this case, PS is the structural phase and poly(ethylene oxide) (PEO) is the transporting phase. The authors define a normalized conductivity, σ_n as

$$\sigma_n = \frac{\sigma}{f\phi_{\text{trans}}\sigma_o} \quad (7)$$

where f is the same morphology factor introduced in eq 4, ϕ_{trans} is the volume fraction of the transporting PEO microphase, and σ_o is the conductivity of the pure homopolymer PEO. The Flory–Huggins interaction parameter between PS and PEO at 80 °C is 0.048.^{34,35} We have used this value to obtain σ_n as a function of χN for SEO/LiTFSI, and the results are given in Table 4.

The triangles in Figure 8a represent the data in Table 4. It is evident that the dependence of both normalized ethanol permeability and normalized ionic conductivity in styrene-containing block copolymers on χN is similar. In other words, the impedance to transport in rubbery block copolymer microphases due to the presence of glassy PS segments is independent of the nature of the species being transported. Ganesan et al. provide a quantitative framework for describing

Table 4. Morphology Factors (f), χN , and Microphase-Separated Morphology of SEO Copolymers

name	f	χN	morphology
SEO13.7-57	2/3	10.8	lamellar
SEO32-50	2/3	25.1	lamellar
SEO60-40	2/3	44.6	lamellar
SEO71-44	2/3	55.8	lamellar
SEO94-57	2/3	73.5	lamellar
SEO123-55	2/3	96.4	lamellar
SEO172-57	2/3	134.5	lamellar

the effect of χN on transport through block copolymers.³⁶ The results in Figure 8a are consistent with this framework.

The dependence of $P_{W,n}$ on χN is qualitatively different from that of $P_{E,n}$ on χN . As seen in Figure 8b, $P_{W,n}$ appears to be independent of χN , and values of $P_{W,n}$ scatter between 0.7 and 1.2. It appears that the transport of water molecules through rubbery domains is not affected by the presence of glassy PS segments. We do not know the reason for the qualitative differences between $P_{E,n}$ and $P_{W,n}$.

4. CONCLUSIONS

A series of SDS triblock copolymers were synthesized by combination of sequential anionic polymerization and coupling chemistry. Our study covers polymers with PDMS volume fractions ranging from 0.59 to 0.83 and total molecular weights ranging from 55 to 150 kg/mol. Transport through membranes of these materials was studied using an 8 wt % ethanol concentration as the feed in a pervaporation apparatus. The permeability of ethanol through these membranes, determined from the pervaporation experiments, was consistent with a simple model for transport through microphase separated systems. We defined a normalized permeability to account for differences in the volume fraction of the transporting phase and morphology. The normalized permeability of ethanol through SDS membranes is independent of PDMS volume fraction and total molecular weight. In a previous paper, we studied pervaporation of the same ethanol/water mixture through SBS membranes.¹³ The normalized permeability of ethanol through SBS membranes was independent of PBD volume fraction but was strong function of total molecular weight. We propose that this qualitative difference between SDS and SBS membranes is due to the difference in χ , the Flory–Huggins interaction parameter that controls microphase separation in these systems. When χN is <100, the transporting PBD microphase contain glassy PS segments, and this slows down the transport of ethanol molecules and values of normalized permeability significantly below unity are obtained. Normalized ethanol permeability in both SBS and SDS membranes approaches unity when χN exceeds 100. This is attributed to the absence of PS segments in the transporting microphases. We demonstrate similarities between ethanol permeation and ionic conductivity in block copolymer membranes. Surprisingly, normalized water permeability through both SDS and SBS membranes appears to be independent of χN . Further work is needed to determine the underpinnings of this observation.

■ AUTHOR INFORMATION

Corresponding Author

*E-mail: nbalsara@berkeley.edu.

Notes

The authors declare no competing financial interest.

■ ACKNOWLEDGMENTS

This research was supported by the Energy Biosciences Institute (EBI), University of California at Berkeley. We thank Drs. Amit Gokhale and Steve Pietsch for their feedback in fermentation compositions. We thank Alex Teran for his help with the conductivity data. The SAXS measurements were performed at the Advanced Light Source at LBNL, supported by the Director, Office of Science, Office of Basic Energy Sciences, of the U.S. Department of Energy under Contract DE-AC02-05CH11231.

■ REFERENCES

- (1) Vane, L. M. *J. Chem. Technol. Biotechnol.* **2005**, *80*, 603.
- (2) Wijmans, J. G.; Baker, R. W. *J. Membr. Sci.* **1995**, *107*, 1.
- (3) Schafer, T.; Bengtson, G.; Pingel, H.; Boddeker, K. W.; Crespo, J. *Biotechnol. Bioeng.* **1999**, *62*, 412.
- (4) Shao, P.; Huang, R. Y. M. *J. Membr. Sci.* **2007**, *287*, 162.
- (5) Nam, S. Y.; Lee, Y. M. *J. Membr. Sci.* **1997**, *135*, 161.
- (6) Devi, D. A.; Smitha, B.; Sridhar, S.; Aminabhavi, T. M. *J. Membr. Sci.* **2005**, *262*, 91.
- (7) Fritz, L.; Hofmann, D. *Polymer* **1997**, *38*, 1035.
- (8) Wang, Y. C.; Fan, S. C.; Lee, K. R.; Li, C. L.; Huang, S. H.; Tsai, H. A.; Lai, J. Y. *J. Membr. Sci.* **2004**, *239*, 219.
- (9) Mohammadi, T.; Aroujalian, A.; Bakhshi, A. *Chem. Eng. Sci.* **2005**, *60*, 1875.
- (10) Xiangli, F. J.; Chen, Y. W.; Jin, W. Q.; Xu, N. P. *Ind. Eng. Chem. Res.* **2007**, *46*, 2224.
- (11) Xiangli, F. J.; Wei, W.; Chen, Y. W.; Jin, W. Q.; Xu, N. P. *J. Membr. Sci.* **2008**, *311*, 23.
- (12) Jha, A. K.; Chen, L.; Offeman, R. D.; Balsara, N. P. *J. Membr. Sci.* **2011**, *373*, 112.
- (13) Jha, A. K.; Tsang, S. L.; Ozcam, A. E.; Offeman, R. D.; Balsara, N. P. *J. Membr. Sci.* **2012**, *401*, 125.
- (14) Young-Hye, L.; McCloskey, B. D.; Sooriyakumaran, R.; Vora, A.; Freeman, B.; Nassar, M.; Hedrick, J.; Nelson, A.; Allen, R. *J. Membr. Sci.* **2011**, *372*, 285.
- (15) Scovazzo, P.; Kieft, J.; Finan, D. A.; Koval, C.; DuBois, D.; Noble, R. *J. Membr. Sci.* **2004**, *238*, 57.
- (16) Fornes, T. D.; Yoon, P. J.; Keskkula, H.; Paul, D. R. *Polymer* **2001**, *42*, 9929.
- (17) Sudre, G.; Inceoglu, S.; Cotanda, P.; Balsara, N. P. *Macromolecules* **2013**, *46*, 1519.
- (18) Yuan, R.; Teran, A. A.; Gurevitch, I.; Mullin, S. A.; Wanakule, N. S.; Balsara, N. P. *Macromolecules* **2013**, *46*, 914.
- (19) Javier, A. E.; Patel, S. N.; Hallinan, D. T.; Srinivasan, V.; Balsara, N. P. *Angew. Chem., Int. Ed.* **2011**, *50*, 9848.
- (20) Elabd, Y. A.; Walker, C. W.; Beyer, F. L. *J. Membr. Sci.* **2004**, *231*, 181.
- (21) Hadjichristidis, N.; Pitsikalis, M.; Pispas, S.; Iatrou, H. *Chem. Rev.* **2001**, *101*, 3747.
- (22) Maheshwari, S.; Tsapatsis, M.; Bates, F. S. *Macromolecules* **2007**, *40*, 6638.
- (23) Eitouni, H. B.; Balsara, N. P. In *Physical Properties of Polymers Handbook*; Mark, J. E., Ed.; Springer: New York, 2006.
- (24) Wijmans, J. G.; Baker, R. W. *J. Membr. Sci.* **1993**, *79*, 101.
- (25) Baker, R. W.; Wijmans, J. G.; Huang, Y. *J. Membr. Sci.* **2010**, *348*, 346.
- (26) Gmehling, J.; Onken, U.; Arlt, W.; Rarey-Nies, J. R. *Vapor-Liquid Equilibrium Data Collection*; Dechema: Flushing, NY, 1988.
- (27) Mach, P.; Pindak, R.; Levelut, A. M.; Barois, P.; Nguyen, H. T.; Baltes, H.; Hird, M.; Toyne, K.; Seed, A.; Goodby, J. W.; Huang, C. C.; Furenliid, L. *Phys. Rev. E* **1999**, *60*, 6793.
- (28) Baker, R. W.; Wijmans, J. G.; Huang, Y. *J. Membr. Sci.* **2010**, *348*, 346.
- (29) Buonomenna, M. G.; Golemme, G.; Tone, C. M.; De Santo, M. P.; Ciuchi, F.; Perrotta, E.; Zappone, B.; Galiano, F.; Figoli, A. *J. Membr. Sci.* **2011**, *385–386*, 162.
- (30) Yoshikawa, M.; Wano, T.; Kitao, T. *J. Membr. Sci.* **1994**, *89*, 23.
- (31) Vane, L. M.; Namboodiri, V. V.; Bowen, T. C. *J. Membr. Sci.* **2008**, *308*, 230.
- (32) Cochran, E. W.; Garcia-Cervera, C. J.; Fredrickson, G. H. *Macromolecules* **2006**, *39*, 4264.
- (33) Helfand, E.; Wasserman, Z. R. *Macromolecules* **1976**, *9*, 879.
- (34) Zhu, L.; Cheng, S. Z. D.; Calhoun, B. H.; Ge, Q.; Quirk, R. P.; Thomas, E. L.; Hsiao, B. S.; Yeh, F.; Lotz, B. *Polymer* **2001**, *42*, 5829.
- (35) Cochran, E. W.; Morse, D. C.; Bates, F. S. *Macromolecules* **2003**, *36*, 782.
- (36) Ganesan, V.; Pyramitsyn, V.; Bertoni, C.; Shah, M. *ACS Macro Lett.* **2012**, *1*, 513.